Full Length Article

Neurotoxicity screening of new psychoactive substances (NPS): Effects on neuronal activity in rat cortical cultures using microelectrode arrays (MEA)

Anne Zwartsen[a,b], Laura Hondebrink[b], Remco HS Westerink[a,*]

[a] *Neurotoxicology Research Group, Division Toxicology, Institute for Risk Assessment Sciences (IRAS), Faculty of Veterinary Medicine, Utrecht University, Utrecht, The Netherlands*
[b] *Dutch Poisons Information Center (DPIC), University Medical Center Utrecht, Utrecht University, Utrecht, The Netherlands*

A B S T R A C T

While the prevalence and the use of new psychoactive substances (NPS) is steadily increasing, data on pharmacological, toxicological and clinical effects is limited. Considering the large number of NPS available, there is a clear need for efficient *in vitro* screening techniques that capture multiple mechanisms of action. Neuronal cultures grown on multi-well microelectrode arrays (mwMEAs) have previously proven suitable for neurotoxicity screening of chemicals, pharmaceuticals and (illicit) drugs. We therefore used rat primary cortical cultures grown on mwMEA plates to investigate the effects of eight NPS (PMMA, α-PVP, methylone, MDPV, 2C-B, 25B-NBOMe, BZP and TFMPP) and two 'classic' illicit drugs (cocaine, methamphetamine) on spontaneous neuronal activity.

All tested drugs rapidly and concentration-dependently decreased the weighted mean firing rate (wMFR) and the weighted mean burst rate (wMBR) during a 30 min acute exposure. Of the 'classic' drugs, cocaine most potently inhibited the wMFR (IC_{50} 9.8 μM), whereas methamphetamine and the structurally-related NPS PMMA were much less potent (IC_{50} 100 μM and IC_{50} 112 μM, respectively). Of the cathinones, MDPV and α-PVP showed comparable IC_{50} values (29 μM and 21 μM, respectively), although methylone was 10-fold less potent (IC_{50} 235 μM). Comparable 10-fold differences in potency were also observed between the hallucinogenic phenethylamines 2C-B (IC_{50} 27 μM) and 25B-NBOMe (IC_{50} 2.4 μM), and between the piperazine derivatives BZP (IC_{50} 161 μM) and TFMPP (IC_{50} 19 μM). All drugs also inhibited the wMBR and concentration-response curves for wMBR and wMFR were comparable.

For most drugs, IC_{50} values are close to the estimated human brain concentrations following recreational doses of these drugs, highlighting the importance of this efficient *in vitro* screening approach for classification and prioritization of emerging NPS. Moreover, the wide range of IC_{50} values observed for these and previously tested drugs of abuse, both within and between different classes of NPS, indicates that additional investigation of structure-activity relationships could aid future risk assessment of emerging NPS.

© 2018 The Authors. Published by Elsevier B.V. This is an open access article under the CC BY license (http://creativecommons.org/licenses/by/4.0/).

1. Introduction

Over the past 5 years, the proportion of the general population (15–64 years) that used a drug at least once has been stable at approximately 5% (UNODC, 2017). The most widely used class of drugs remains cannabinoids, although its use is stabilizing or even declining in parts of Europe. The second most used class of drugs are the amphetamines and their use, particularly methamphetamine, has been increasing in some European countries (UNODC, 2017). The use of amphetamines accounts for a considerable share of the estimated 28 million 'healthy' life years lost by drug use in 2015 (disability-adjusted life years (DALYs)). Of all amphetamines, methamphetamine contributes most to the global burden of disease, and an increasing number of methamphetamine users are seeking treatment (UNODC, 2017).

New psychoactive substances (NPS), also known as 'legal highs', 'bath salts' or 'research chemicals', appeared on the drug market around a decade ago. Even though they account for only a small

* Corresponding author at: Neurotoxicology Research Group, Division Toxicology, Institute for Risk Assessment Sciences (IRAS), Faculty of Veterinary Medicine, Utrecht University, P.O. Box 80.177, Utrecht NL-3508 TD, The Netherlands.
E-mail address: r.westerink@uu.nl (R.H. Westerink).

proportion of the market, NPS encompass a group of over 700 different substances. These potentially harmful drugs are manufactured to have intended effects comparable to those of illegal drugs like amphetamine, lysergic acid diethylamide (LSD), ketamine and 3,4-methylenedioxymethamphetamine (MDMA). The potential of NPS to cause harm is at least partly due to the inexperience of users with regards to *e.g.*, dosing or routes of administration. In addition, the pharmacological and toxicological mechanisms of these drugs are often not fully elucidated (Hondebrink et al., 2018). Drug users also may have been taken NPS unknowingly, as NPS were sometimes used as adulterants in more commonly used illicit drugs (EMCDDA, 2016). For example, in the Netherlands high doses of *para*-methoxymethamphetamine (PMMA) were detected in ecstasy tablets, for which health alerts were issued (Van der Gouwe and Rigter, 2017). Over the last years, however, NPS are becoming a 'drug of choice' instead of being adulterants (UNODC, 2017). Although around 100 NPS are reported to monitoring centers for the first time annually, only a core group of over 80 NPS have been reported every year since 2009. Some of the NPS that stayed on the market, like alpha-pyrrolidinovalerophenone (α-PVP), benzylpiperazine (BZP), 3,4-methylenedioxypyrovalerone (MDPV), mephedrone, methylone and PMMA, have now been classified as illegal drugs by authorities in several countries including the UK, Canada, Australia and many European countries (UNODC, 2017).

In 2014, the life-time prevalence of NPS use for young European adults (15–24 years) was 8% (European commission, 2014). In vulnerable groups (homeless, young people, people with mental health issues, men who sleep with men, and people who inject drugs) this number was as high as 59% (MacLeod et al., 2016). In addition, according to a survey among NPS users, 30% had used nine or more NPS during the last five years compared to 15% who only used one NPS. Further, 76% of NPS users who tried more than one NPS were inclined to use NPS from different classes (Soussan and Kjellgren, 2016).

Even though NPS are becoming increasingly popular, surveys have shown that most young people think that regular NPS use has a high health risk. However, only 50% of young people think that high risks are involved when NPS are used only once or twice, while 10% think there is no or a low risk (European Commission, 2014). Nevertheless, the emergence of NPS has been associated with severe intoxications and fatalities (UNODC, 2017). Compounds mimicking the hallucinogenic effects of LSD (which are therefore sometimes sold as LSD), for instance 2C-B and especially its NBOMe derivatives, have caused intoxications and even fatalities (Wood et al., 2015). In addition, in 2015 α-PVP was linked to 63 deaths and over 1800 hospital emergency admissions in only one county in Florida (ACC, 2015).

Analogues to' classic' illicit drugs, most NPS exert their intended effects at least partly by increasing brain monoamine levels. Illicit drugs and NPS can increase dopamine, norepinephrine and serotonin levels by blocking and/or reversing the dopamine, norepinephrine and serotonin reuptake transporters (Zwartsen et al., 2017; Rickli et al., 2015; Simmler et al., 2013). In addition, several other mechanisms of action are contributing to the effects of NPS, including (ant)agonistic effects on multiple neurotransmitter receptors (*e.g.* GABA$_A$, NMDA, 5-HT$_2$ and ACh) and/or inhibition of ion channels (*e.g.* voltage-gated calcium channels) (see Hondebrink et al., 2018 for review).

While knowledge of effects of NPS on single endpoints is valuable, the increasing number of NPS illustrates the need for efficient *in vitro* screening techniques that capture multiple mechanisms of action. Recently, neuronal cultures grown on microelectrode arrays (MEAs) have proven to be suitable for neurotoxicity screening of pharmaceuticals, toxins, chemicals and (illicit) drugs (Strickland et al., 2018; Vassallo et al., 2017;

Hondebrink et al., 2016; Nicolas et al., 2014; Valdivia et al., 2014; McConnell et al., 2012; Puia et al., 2012). Using this method, valuable information can be obtained quickly by investigating effects on neuronal activity as an integrated endpoint of underlying effects on all targets affected within the neuronal network, including different ion channels, neurotransmitter receptors and compensatory mechanisms.

As the prevalence and use of NPS is continuously increasing, we investigated the acute effects of 10 NPS and' classic' illicit drugs on spontaneous neuronal activity at human relevant concentrations. The tested NPS and illicit drugs were chosen based on continued presence on the drug market. Compounds were categorized based on chemical similarities for characterization purposes; *i.e.* amphetamine-type stimulants (methamphetamine and PMMA), hallucinogenic phenethylamines (2C-B and 25B-NBOMe), cathinones (methylone, MDPV and α-PVP), piperazines (BZP and TFMPP) and others (cocaine).

2. Methods

2.1. Chemicals

D-Methamphetamine, methylone, PMMA, 2C-B, 25B-NBOMe, α-PVP, MDPV, BZP and TFMPP hydrochloride salts (purity > 98.5%) were purchased from Lipomed (Weil am Rhein, Germany). Cocaine (purity > 98.5) was obtained from Spruyt Hillen (IJsselstein, the Netherlands) (for IUPAC names see Table 1). Neurobasal-A (NBA) medium, L-glutamine (200 mM), Penicillin/streptomycin (5000 U/mL/5000 mg/mL), fetal bovine serum (FBS) and B-27 supplement (without vitamin A) were obtained from Life Technologies (Bleiswijk, The Netherlands). All other chemicals, unless otherwise noted, were purchased from Sigma–Aldrich (Zwijndrecht, The Netherlands). Stock solutions of drugs were prepared at the day of the experiment in FBS medium, unless otherwise specified.

2.2. Neuronal cultures

Rat pups born of timed-pregnant Wistar rats (Envigo, Horst, the Netherlands) were used on postnatal day 0–1 to isolate cortical neurons. Cortical cultures were prepared as described previously (Hondebrink et al., 2016). Briefly, cortices were isolated, minced with scalpels, triturated and filtered through a 100 μm mesh (EASY-strainer, Greiner) to get a homogenous cell suspension in dissection medium consisting of 500 mL Neurobasal-A supplemented with 14 g sucrose, 1.25 mL L-glutamine (200 mM), 5 mL glutamate (3.5 mM), 5 mL penicillin/streptomycin and 50 mL FBS (osmolarity of ~330 mOsm). Subsequently, cells were centrifuged for 5 min at 800 rpm, the supernatant was removed and the pellet was resuspended using 1 mL of dissection medium per rat brain and diluted to a cell suspension containing 2×10^6 cells/mL. Next, a 50 μL drop of cell suspension was added to each well (1×10^5 cells/well) of a 48-wells MEA plate (Axion BioSystems Inc, Atlanta, USA, M768-GL1-30Pt200) coated with PEI (0.1% PEI solution in borate buffer (24 mM sodium borate/ 50 mM boric acid in Milli-Q adjusted to pH 8.4)). Cells were allowed to attach for 2 h at 37 °C, 5% CO$_2$/95% air atmosphere before 450 μL dissection medium was added to each well. The day after the isolation (day *in vitro* 1; DIV1) 450 μL/well of the dissection medium was replaced with the same amount of glutamate medium (500 mL NBA medium, 14 g sucrose, 1.25 mL L-glutamine (200 mM), 5 mL glutamate (3.5 mM), 5 mL penicillin/streptomycin and 10 mL B-27, pH 7.4 (osmolarity of ~330 mOsm)). At DIV4, 450 μL/well glutamate medium was replaced with 450 μL/well FBS medium (glutamate-free dissection medium (osmolarity of ~330 mOsm)). Cultures were kept in FBS medium at 37 °C, 5% CO$_2$/95% air atmosphere until use at DIV9-10.

Table 1
Characteristics of the tested illicit drugs and NPS.

Group	Drug	Synonyms	IUPAC Name	CAS number	Sources	Exposure medium	Conc. range	Exposure volume
Amphetamine-type stimulants	Meth-amphetamine	Crystal, Meth, Speed, Crank	(2S)-N-methyl-1-phenylpropan-2-amine	537-46-2	Lipomed	FBS# medium	1-1000 µM	5 µL
	PMMA	Red Mitsubishi, 4-MMA	1-(4-methoxyphenyl)-N-methylpropan-2-amine	22331-70-0	Lipomed	FBS medium	10-1000 µM	5 µL
Cathinones	Methylone	Explosion, bk-MDMA, MDMC,	1-(1,3-benzodioxol-5-yl)-2-(methylamino)propan-1-one	186028-79-5	Lipomed	FBS medium	1-1000 µM	5 µL
	MDPV	Peevee, Magic, Super coke, MP3/MP4	1-(1,3-benzodioxol-5-yl)-2-pyrrolidin-1-ylpentan-1-one	687603-66-3	Lipomed	FBS medium	1-1000 µM	55 µL*
	α-PVP	Flakka, Gravel, Grind	1-phenyl-2-pyrrolidin-1-ylpentan-1-one	14530-33-7	Lipomed	FBS medium	1-300 µM*	5 µL
Hallucinogenic phenethylamines	2C-B	Venus, Bromo, Erox, Bees, Nexus	2-(4-bromo-2,5-di methoxyphenyl)ethanamine	66142-81-2	Lipomed	FBS medium	1-300 µM*	5 µL
	25B-NBOMe	N-Bomb	2-(4-bromo-2,5-dimethoxyphenyl)-N-[(2-methoxyphenyl)methyl]ethanamine	1026511-90-9	Lipomed	10% HBSS/90% NB-A medium	0.01-30 µM*	55 µL*
Piperazines	BZP	Benny bear, Flying Angel, A2, Nemesis, PEP, X4, Legal E, Party Pill, Frenzy	1-benzylpiperazine	2759-28-6	Lipomed	FBS medium	1-1000 µM	5 µL
	TFMPP		1-[3-(trifluoromethyl)phenyl]piperazine	15532-75-9	Lipomed	FBS medium	1-1000 µM	5 µL
Other	Cocaine	C, Coke, Crack, Blow, Bump, Snow	methyl(1S,3S,4R,5R)-3-benzoyloxy-8-methyl-8-azabicyclo[3.2.1]octane-4-carboxylate	50-36-2	Spruyt Hillen	FBS medium	1-100 µM	5 µL

'Exposure volume' indicates the volume that is added to each MEA well during exposure recording. *Due to solubility issues with these NPS, the exposure volume, maximum concentration and/or exposure medium were different. #FBS medium: 500 mL Neurobasal-A medium supplemented with 14 g sucrose, 1.25 mL L-glutamine (200 mM), 5 mL penicillin/streptomycin and 50 mL Fetal bovine serum, HBSS: Hanks' balanced salt solution, NB-A: Neural basal A medium.

Animal experiments were performed in agreement with Dutch law, the European Community directives regulating animal research (2010/63/EU) and approved by the Ethical Committee for Animal Experiments of Utrecht University. All efforts were made to minimize the number of animals used and their suffering.

2.3. MEA recordings

At DIV9-10, mwMEA plates (48 wells with 16 individual embedded nanotextured gold microelectrodes per well (∼40–50 µm diameter; 350 µm center-to-center spacing)) were placed in a Maestro 768-channel amplifier with integrated heating system, temperature controller and data acquisition interface (Axion BioSystems Inc, Atlanta, USA) to record spontaneous neuronal activity. Prior to each recording, the plate was allowed to equilibrate for 2–5 min. Baseline spontaneous neuronal activity was recorded for 30 min. Following the baseline recording, all wells were exposed individually by manually pipetting 5 µL FBS medium with or without (control) drugs, under sterile conditions. Next, a 30 min exposure recording was started to determine the effects of drugs on spontaneous neuronal activity. The following substances and concentrations were tested: methamphetamine, methylone, BZP and TFMPP (1–1000 µM), 2C-B and α-PVP (1–300 µM),

cocaine (1–100 µM) and PMMA (10–1000 µM; also see Table 1). Due to solubility limitations of MDPV and 25B-NBOMe, wells were exposed individually by manually pipetting 55 µL FBS medium with MDPV (1–1000 µM) or without (control for MDPV), or 55 µL 10% Hanks' balanced salt solution ((HBSS)/90% Neurobasal-A) medium with 25B-NBOMe (1–30 µM) or without (control for 25B-NBOMe; also see Table 1). The tested concentrations for each substance were based on range finding experiments starting with 1, 10 and 100 µM, if solubility allowed. To prevent possible effects of cumulative dosing, including receptor (de)sensitization, each well was exposed to only a single substance at a single concentration. For each experimental condition, primary cultures from at least two different isolations (average 4 isolations) were used and tested in at least 5 plates (average 7 plates). The number of wells represents the number of replicates per condition.

2.4. Data analysis and statistics

After recording neuronal activity, raw data files were re-recorded using AxIS spike detector (Adaptive threshold crossing, Ada BandFlt v2) to map the spikes. Spikes were defined by >7xSD of the internal noise level (rms) with a post/pre spike duration of 3.6/2.4 ms of each individual electrode. Spike information was then further analyzed

using NeuroExplorer® (Nex Technologies, Madison (AL), US) and custom-made macros in Excel (for workflow see Fig. 1).

To analyze effects of NPS and illicit drugs on weighted mean firing rate (wMFR) or weighted mean burst rate (wMBR), only wells that contained ≥1 active electrode (with ≥0.1 spike/sec) in the baseline recording were included. On average, each well contained 7 active electrodes. Bursts were defined using the Poisson surprise method (minimum of 10 surprises). All tested drugs induced effects rapidly following exposure and effects lasted the entire exposure recording. The wMFR and wMBR from the last 10 min (most stable timeframe; Hondebrink et al., 2016) of the 30 min exposure recording was therefore used for analysis. Effects of test compounds on wMFR or wMBR were analyzed as follows:

First, the wMFR and wMBR were calculated per well prior to exposure (the reference activity, wMFR$_{baseline}$ or wMBR$_{baseline}$). Next, the wMFR and wMBR were calculated per well following exposure (wMFR$_{exposure}$ or wMBR$_{bexposure}$). Subsequently, wMFR$_{exposure}$ was expressed as a percentage of wMFR$_{baseline}$ (and wMBR$_{exposure}$ vs wMBR$_{baseline}$) of the same well to obtain a treatment ratio (paired comparison, see Fig. 1 for workflow). Treatment ratios were also calculated for control wells that were exposed only to medium during the exposure recording. Then treatment ratios (wMFR$_{exposure}$ as a percentage of wMFR$_{baseline}$ or wMBR$_{exposure}$ as a percentage of wMBR$_{baseline}$) were sorted per condition per compound (e.g., 10 μM methylone). Wells with treatment ratios > mean ± 2xSD (of their respective condition) were considered outliers and excluded (4.3%). Finally, the average
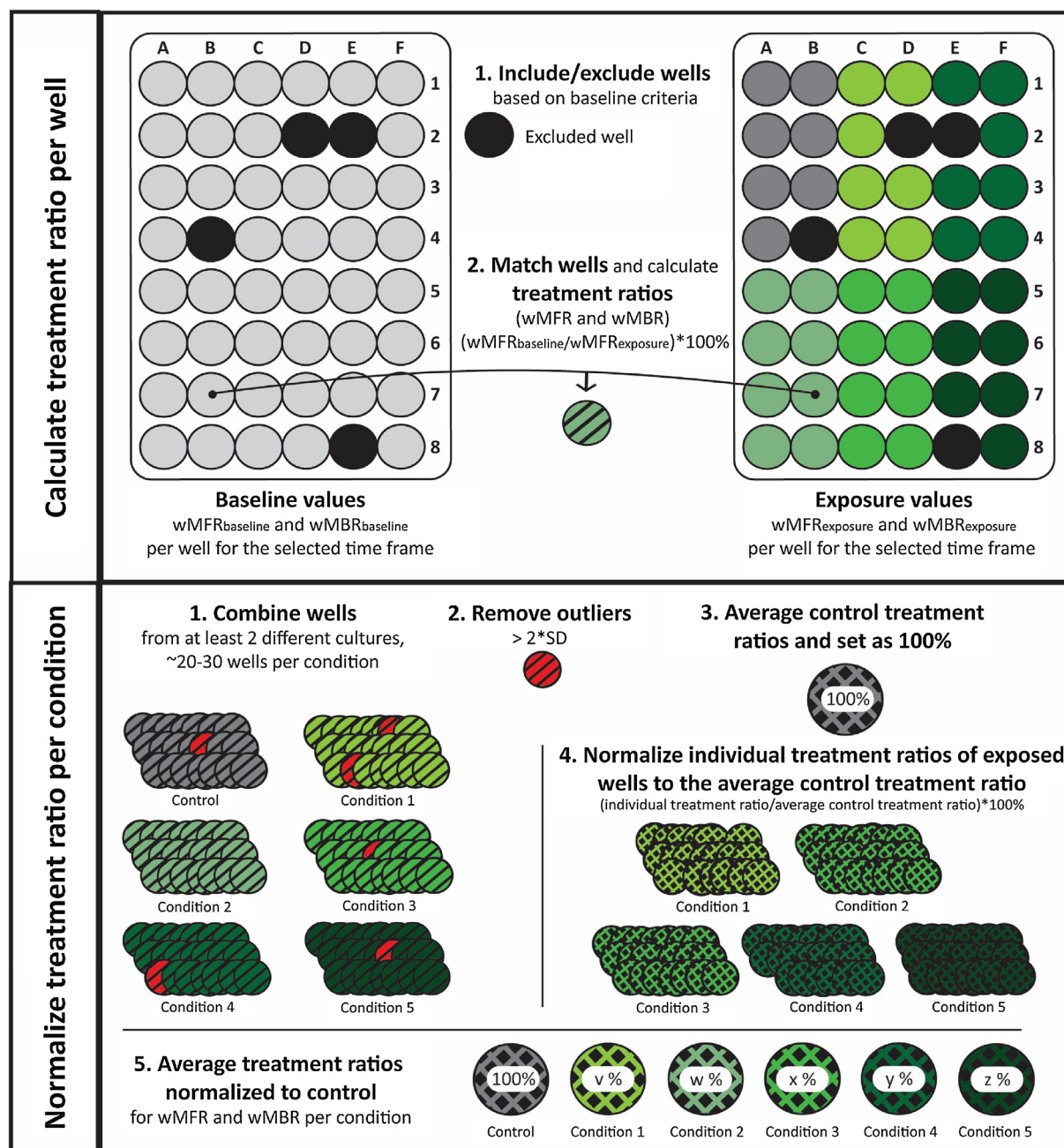

Fig. 1. Schematic illustration of the collection and analysis of neuronal network activity. Spontaneous network activity is recorded for 30 min using the Maestro and Axion Biosystems hardware. Using Axion software, recordings were re-recorded to generate spike count files. Subsequently, active baseline wells were selected in the selected timeframes using NeuroExplorer software and the listed criteria. Then, custom-made macro's were used to calculate treatment ratio's, remove outliers, and finalize calculations. wMFR: weighted mean firing rate, wMBR: weighted mean burst rate.

control treatment ratio was set to 100% and treatment ratios of individual exposed wells were normalized to the average treatment ratio of medium control wells. Treatment ratios of exposed wells were averaged per condition per compound and used for further statistical analysis. To determine the robustness of the selection criteria for inclusion of active wells, a separate analysis was performed in which only wells with ≥ 9 active electrodes were included (also see Supplemental Results).

GraphPad Prism software (v6, GraphPad Software, La Jolla CA, USA) was used for data analysis. Non-linear regressions were used to calculate IC_{50} values. When applicable, a one-way ANOVA followed by a *post-hoc* Dunnet's test was used to compare treatment ratios in drug-exposed wells to treatment ratios in control wells. Effects on neuronal activity (wMFR and wMBR) were considered relevant when the effect was statistically significant ($p < 0.05$) and $\geq 30\%$. The lowest observed effect concentration (LOEC) was defined as the lowest concentration that induced a relevant inhibiting effect. Data is shown as mean $\pm$ SEM for n_{wells}, N_{plates} from at least two different isolations.

2.5. Calculation of estimated human brain concentrations following recreational drug use

The estimated human brain concentration range was calculated for methamphetamine, cocaine and PMMA according to Zwartsen et al. (2017). Estimated human brain concentrations of other substances were obtained from Hondebrink et al., 2018. In short, a recreational methamphetamine blood concentration range of 0.05–20 μM was established based on data from literature on apprehended drivers, people arrested for criminal activity or partygoers (Jones et al., 2008; Melega et al., 2007; Irvine et al., 2006). The blood concentration range was multiplied by the brain partition factor (1.0–2.8), which was based on 11 human case reports on lethal methamphetamine exposures that reported blood and brain concentrations (Kiely et al., 2009; Chaturvedi et al., 2004; Saito et al., 1996; Hara et al., 1986; Kojima et al., 1984). The estimated brain concentration after recreational use was calculated to be 0.05–56 μM for methamphetamine.

The reported blood concentration after recreational cocaine use was between 0.01–3.0 μM (Senna et al., 2010; Steentoft et al., 2010). An estimated brain concentration of 0.02–30 μM was determined by multiplying the recreational blood concentration by a brain partition factor of 1.7–10, which was based on human blood and brain concentrations obtained post-mortem (Brajkovic et al., 2016; Giroud et al., 2004; Kiszka and Madro, 2004; Poklis et al., 1987, 1985).

Blood concentrations after (un)intentional consumption of PMMA found in literature ranged from 0.1–3.6 μM (Vevelstad et al., 2012). Based on rat studies (serum to brain and plasma to brain) a brain partition factor of 4.1–16 (Pálenícek et al., 2011; Rohanova and Balikova, 2009) was used to determine an estimated brain concentration of 0.4–58 μM.
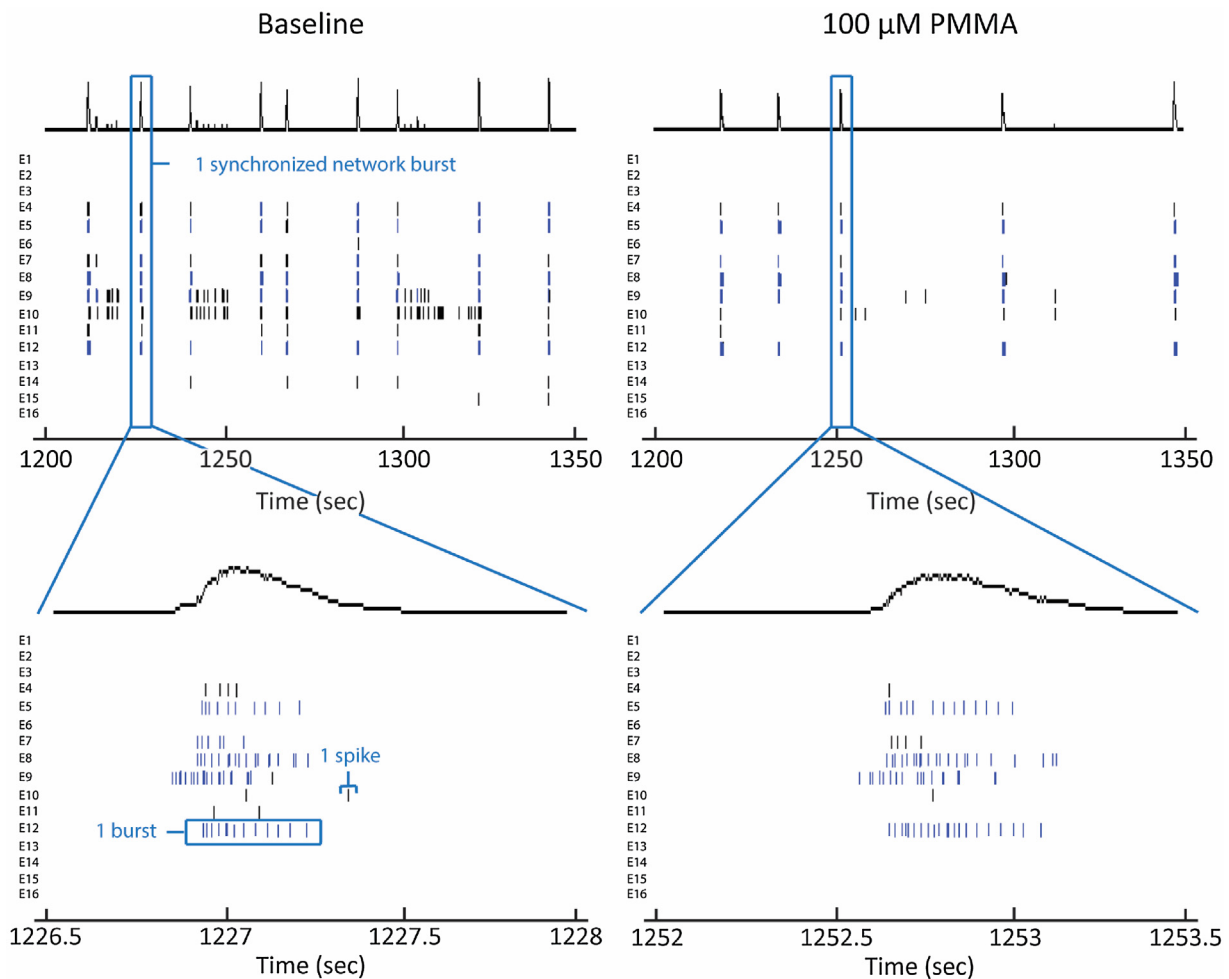

Fig. 2. Frequency histogram and raster plot of a representative MEA recording. Graph depicts a 150 s time window with a frequency histogram (top trace) and raster plot of neuronal activity recorded from 11 active electrodes (out of 16 electrodes in total, indicated as E1-E16) in a single well before (baseline, left) and after exposure to 100 μM PMMA (right). Inserts (bottom) show a magnification of 1.5 s of the recording, highlighting a synchronized network burst. Following exposure to PMMA, the number of (synchronized network) bursts is decreased (top right), while the number of spikes within in a burst is largely unaffected (bottom right).
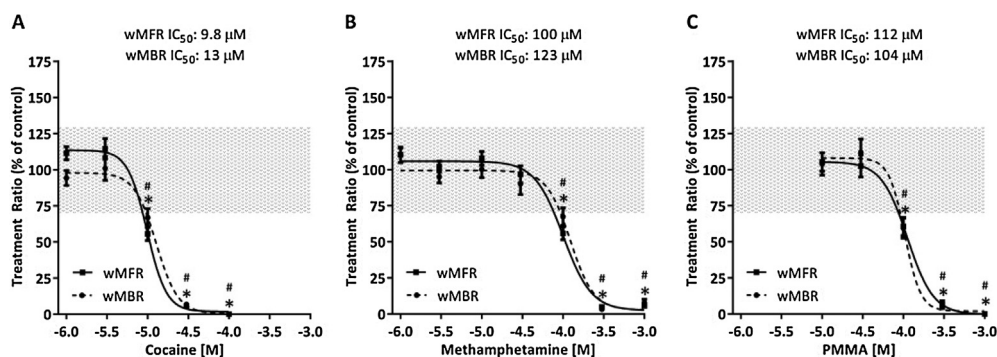
Fig. 3. Concentration-response curves of cocaine and two amphetamine-type stimulants for the weighted mean firing rate (wMFR, solid line) and the weighted mean burst rate (wMBR, dotted). (A) Cocaine (wMFR n_{wells} = 25–30, N_{plates} = 6–8, wMBR n_{wells} = 24–28, N_{plates} = 6–8), (B) methamphetamine (wMFR n_{wells} = 23–29, N_{plates} = 3–8, wMBR n_{wells} = 22–28, N_{plates} = 3–8) and (C) PMMA (wMFR n_{wells} = 25–32, N_{plates} = 5–8, wMBR n_{wells} = 23–30, N_{plates} = 5–8). Neuronal activity is depicted as the mean treatment ratio ± SEM (wMFR$_{exposure}$/wMFR$_{baseline}$ and wMBR$_{exposure}$/wMBR$_{baseline}$ as % of control wells). Effects ≤ 30% (*i.e.* variation of medium control) are considered not to be of (toxicological) relevance, as is depicted by the grey area. * (wMFR) and # (wMBR) indicate a relevant and statistically significant ($p > 0.05$) effect.

3. Results

3.1. Effect of drugs and NPS on neuronal activity

Spontaneous electrical activity in primary rat cortical cultures develops within the first week of *in vitro* culture and optimal activity is reached around DIV10 (Dingemans et al., 2016). We therefore exposed rat cortical cultures on DIV9-10 to determine the effects of two' classical' illicit drugs and eight NPS on neuronal activity. Following baseline recording, active wells were exposed for 30 min to different concentrations of cocaine, methamphetamine, PMMA, methylone, MDPV, α-PVP, 2C-B, 25B-NBOMe, BZP and TFMPP. Each well was exposed to only a single concentration of test compound to prevent possible effects of cumulative dosing, including receptor (de)sensitization. Concentration-response curves for effects on wMFR were obtained by comparing the treatment ratios (wMFR$_{exposure}$ *vs* wMFR$_{baseline}$) of wells exposed to different concentrations of a particular drug to the treatment ratio of the control wells on matching plates. While wMFR is a sensitive and robust parameter that is suitable for evaluation of chemical effects on neuronal activity (Novellino et al., 2011), it may not adequately reflect changes in the pattern of spike activity such as changes in the weighted mean burst rate (wMBR). Rat primary cortical networks grown on MEAs show distinct bursts that are synchronized over the entire network in the well, as shown in Fig. 2. Analogous to wMFR, we therefore also constructed concentration-response curves for the effects of the different

drugs on wMBR. In general, all drugs concentration-dependently inhibited neuronal activity (Figs. 3–6).

3.1.1. Cocaine and amphetamine-type stimulants

The amphetamine-type stimulants (ATS) methamphetamine and PMMA inhibited wMFR with IC$_{50}$ values of 100 μM and 112 μM, respectively (Fig. 3). wMBR IC$_{50}$ values (IC$_{50}$ values of 123 and 104 μM, respectively) were comparable to those for wMFR. Cocaine was ~10 times more potent with an wMFR IC$_{50}$ value of 9.8 μM and a wMBR IC$_{50}$ value of 13 μM. Similarly, cocaine completely abolished neuronal activity at a concentration 10 times lower than methamphetamine or PMMA. The inhibitory LOEC values (both wMFR and wMBR) for cocaine, methamphetamine and PMMA were close to IC$_{50}$ values and were 10 μM, 100 μM and 100 μM, respectively.

3.1.2. Cathinones

The cathinones MDPV and α-PVP inhibited wMFR with IC$_{50}$ values of 29 μM and 21 μM, respectively (Fig. 4). The IC$_{50}$ values for wMBR were 28 μM for α-PVP and 14 μM for MDPV. Both NPS completely abolished neuronal activity at 100 μM. Methylone was ~10 times less potent compared to MDPV and α-PVP (wMFR IC$_{50}$ value of 235 μM and wMBR IC$_{50}$ value of 246 μM) and completely inhibited neuronal activity at 1 mM. The inhibitory wMFR and wMBR LOEC values for methylone were 300 μM, 100 μM (wMFR) and 30 μM (wMBR) for MDPV and α-PVP had inhibitory LOEC values of 30 μM.
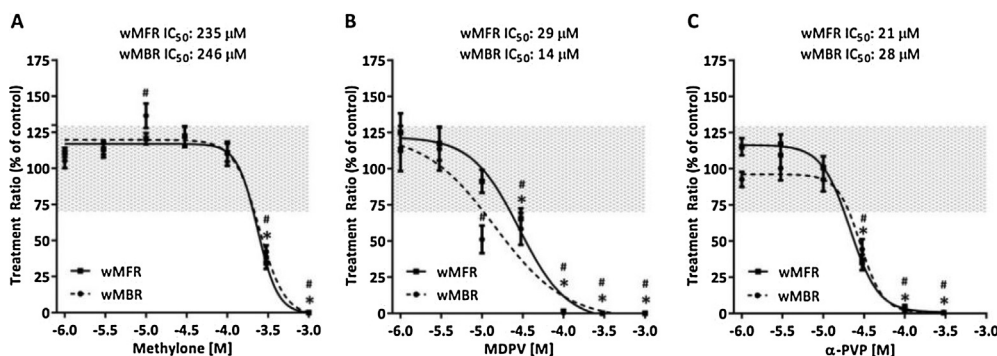

Fig. 4. Concentration-response curves of three cathinones for the weighted mean firing rate (wMFR, solid line) and the weighted mean burst rate (wMBR, dotted). (A) Methylone (wMFR n_{wells} = 18–27, N_{plates} = 4–5, wMBR n_{wells} = 18–29, N_{plates} = 4–5), (B) MDPV (wMFR n_{wells} = 24–31, N_{plates} = 5–6, wMBR n_{wells} = 20–29, N_{plates} = 5–6) and (C) α-PVP (wMFR n_{wells} = 26–33, N_{plates} = 6–8, wMBR n_{wells} = 22–31, N_{plates} = 6–8). Neuronal activity is depicted as the mean treatment ratio ± SEM (change in wMFR$_{baseline}$/wMBR$_{baseline}$ and wMFR$_{exposure}$/wMBR$_{exposure}$ as % of control wells). Effects ≤30% (*i.e.* variation of medium control) are considered not to be of (toxicological) relevance, as is depicted by the grey area. * (wMFR) and # (wMBR) indicate a relevant and statistically significant ($p > 0.05$) effect.
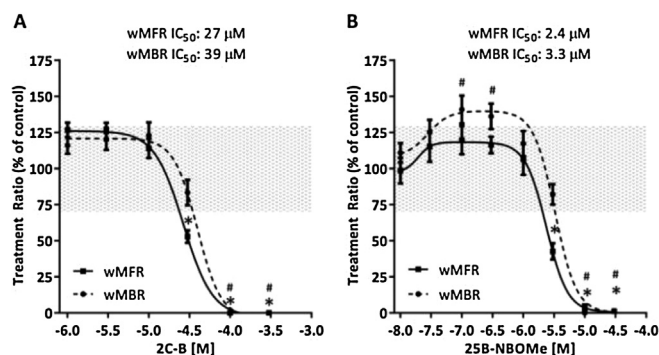
Fig. 5. Concentration-response curves of two hallucinogenic phenethylamines for the weighted mean firing rate (wMFR, solid line) and the weighted mean burst rate (wMBR, dotted). (A) 2C-B (wMFR n_{wells} = 19–29, N_{plates} = 4–5, wMBR n_{wells} = 18–30, N_{plates} = 4–5) and (B) 25B-NBOMe (wMFR n_{wells} = 19–21, N_{plates} = 4, wMBR n_{wells} = 18–21, N_{plates} = 4). Neuronal activity is depicted as the mean treatment ratio ± SEM (change in $wMFR_{baseline}/wMBR_{baseline}$ and $wMFR_{exposure}/wMBR_{exposure}$ as % of control wells). Effects ≤30% (i.e. variation of medium control) are considered not to be of (toxicological) relevance, as is depicted by the grey area. * (wMFR) and # (wMBR) indicate a relevant and statistically significant ($p > 0.05$) effect.
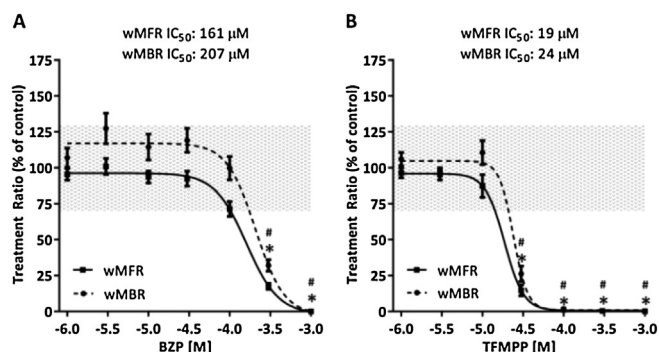

Fig. 6. Concentration-response curves of two piperazines for the weighted mean firing rate (wMFR, solid line) and the weighted mean burst rate (wMBR, dotted). (A) BZP (wMFR n_{wells} = 20–29, N_{plates} = 5–6, wMBR n_{wells} = 19–29, N_{plates} = 5) and (B) TFMPP (wMFR n_{wells} = 24–34, N_{plates} = 4–9, wMBR n_{wells} = 20–33, N_{plates} = 5). Neuronal activity is depicted as the mean treatment ratio ± SEM (change in $wMFR_{baseline}/wMBR_{baseline}$ andw $MFR_{exposure}/wMBR_{exposure}$ as % of control wells). IC$_{50}$ values (μM) are presented with 95% confidence intervals [CI]. Effects ≤30% (i.e. variation of medium control) are considered not to be of (toxicological) relevance, as is depicted by the grey area. * (wMFR) and # (wMBR) indicate a relevant and statistically significant ($p > 0.05$) effect.

3.1.3. Hallucinogenic phenethylamines

The hallucinogenic phenethylamine 25B-NBOMe inhibited both wMFR and wMBR more potently compared to 2C-B (Fig. 5); a 10-fold difference is observed between wMFR IC$_{50}$ values (2.4 μM and 27 μM, respectively) and a 10-fold difference is seen between wMBR IC$_{50}$ values (3.3 μM and 39 μM, respectively). The concentration at which neuronal activity is completely inhibited also showed a 10-fold difference; 10 μM for 25B-NBOMe vs 100 μM for 2C-B. The inhibitory wMFR and wMBR LOEC values for 25B-NBOMe and 2C-B amounted to 3 and 10 μM, and 30 and 100 μM, respectively. Also a significant slight increase in the wMBR is seen at low concentrations of 25B-NBOMe (0.1 and 0.3 μM).

3.1.4. Piperazines

The piperazine derivatives BZP and TFMPP also inhibited wMFR and wMBR in a comparable manner; a 10-fold difference in IC$_{50}$ values was observed between these compounds (wMFR IC$_{50}$ values of 161 μM and 19 μM, respectively, and wMBR IC$_{50}$ values of 207 μM and 24 μM, respectively) (Fig. 6). This difference in IC$_{50}$ values was also reflected in the difference between complete inhibition of the neuronal networks (1 mM and 100 μM,

respectively) and the inhibitory wMFR and wMBR LOEC values for BZP and TFMPP (300 μM and 30 μM, respectively).

3.2. Effects on wMBR

Exposure to NPS or classical drugs thus not only induced a profound decrease in wMFR, but also resulted in a concentration-dependent decrease in wMBR (Figs. 3–6). In general, all drugs show comparable IC$_{50}$ values for wMBR and wMFR (Table 2). Notably, the parallel decline in both wMFR and wMBR may suggests that the total number of spikes within bursts remained largely unaffected.

3.3. Effects of electrode selection based on activity

We have previously shown that the concentration-response curves of a set of drugs were largely independent of the baseline spike frequency. For example, including only electrodes with higher MFR for analysis of drug-induced effects on wMFR (0.1 Hz versus 1 Hz) did not change the concentration-response curves (Hondebrink et al., 2016). We now also investigated if changing the selection criteria for active wells (more active electrodes per well) affects the results. Notably, no difference was observed in the concentration-response curves between analysis with wells with ≥ 1 active electrode and analysis with wells with ≥9 active electrodes (see Supplemental Results), highlighting the robustness of the mwMEA approach.

4. Discussion

We recently used rat cortical cultures grown on mwMEA to derive proof of principle for its usability as an efficient screening tool to determine the effects of (illicit) drugs on spontaneous neuronal activity (Hondebrink et al., 2017, 2016). The present study elaborates on this successful proof of principle by investigating the effects of an additional 10 different illicit drugs and NPS. Analogous to our previous findings, all tested drugs inhibited neuronal activity (weighted mean firing rate (wMFR)) with wMFR IC$_{50}$ values ranging from 2.4 μM for 25B-NBOMe to 234 μM for methylone. A comparable range was observed for inhibition of the weighted mean burst rate (wMBR; IC$_{50}$ 3.3 μM for 25B-NBOMe to IC$_{50}$ 246 μM for methylone). The similarity in concentration-response curves for wMFR and wMBR suggests that the number of spikes per burst may be unaffected (also see sample trace in Fig. 2). Notably, our data also demonstrate that the results are largely independent of the number of active electrodes/well (Supplemental Results). This also implies that implementation of higher throughput 96-well MEA plates (with 8 electrodes/well) or even future 384-well MEA plates (with only 2 electrodes/well) would likely not affect the results if neuronal networks show synchronized activity.

Importantly, the observed broad range of IC$_{50}$ values hints to the possible existence of distinct structure-activity relationships (SARs). By including data from our previous studies, we are able to compare the effects of 16 illicit drugs and NPS from different classes on spontaneous neuronal activity (wMFR; Table 3). Firstly, all amphetamine-type stimulants (amphetamine, methamphetamine, MDMA, PMMA and 4-FA) inhibit the wMFR with IC$_{50}$ values of ~100 μM. Small changes in the chemical structure of this group, like the addition of a fluorine atom, and a methoxy or methylenedioxy structure, do not change their potency to inhibit the wMFR (Table 3 and Fig. 7). Nonetheless, these structural changes might influence distribution and clearance in vivo.

Secondly, the addition of a ketone group to the MDMA structure, resulting in the cathinone methylone, decreases the potency of the compound to inhibit the wMFR 2-fold (IC$_{50}$ values 106 μM vs 234 μM, respectively; Fig. 7). On the other hand, the

Table 2
IC$_{50}$ and LOEC values for the inhibition of the weighted mean firing rate (wMFR) and weighted mean burst rate (wMBR) of 8 NPS and 2 illicit drugs.

Group	Drug	IC$_{50}$ values wMFR (μM)	LOEC values wMFR (μM)	IC$_{50}$ values wMBR (μM)	LOEC values wMBR (μM)
Amphetamine-type stimulants	Methamphetamine	100 [84-117]	100	123 [104-147]	100
	PMMA	112 [94-141]	100	104 [91-131]	100
Cathinones	Methylone	235 [202-264]	300	246 [194-308]	300
	MDPV	29 [18-41]	30	14 [6.6-31]	10
	α-PVP	21 [17-26]	30	28 [23-35]	30
Hallucinogenic phenethylamines	2C-B	27 [24-30]	30	39 [33-48]	100
	25B-NBOMe	2.4 [1.8-3.1]	3	3.2 [2.8-3.9]	3
Piperazines	BZP	161 [129-205]	300	207 [152-288]	300
	TFMPP	19 [16-22]	30	24 [22-26]	30
Other	Cocaine	9.8 [8.7-11]	10	13 [11-15]	10

IC$_{50}$ values (μM) are presented with 95% confidence intervals [CI]. LOEC: lowest observed effect concentration.

Table 3
IC$_{50}$ values for inhibition of weighted mean firing rate (wMFR) and weighted mean burst rate (wMBR) of 11 NPS and 5 illicit drugs compared to the estimated human brain concentration ([brain]). IC$_{50}$ values not within or close to 2 times the estimated human brain concentration are highlighted in grey. [a]: Hondebrink et al., 2016, [b]: Hondebrink et al., 2018, [c]: Hondebrink et al., 2017. MDMA: 3,4-methylenedioxymethamphetamine, 4-FA: 4-fluoroamphetamine, mCPP: (1-(3-chlorophenyl)piperazine), MXE: methoxetamine, for other drugs see Table 1. N.D.: not determined.

Group	Drug	IC$_{50}$ values wMFR (μM)	IC$_{50}$ values wMBR (μM)	[brain] (μM)
Amphetamine-type stimulants	Amphetamine	110[a]	N.D.	0.3-336[b]
	4-FA	113[a]	N.D.	0.1-12[b]
	Methamphetamine	100 [84-117]	123 [104-147]	0.05-56
	PMMA	112 [94-141]	104 [91-131]	0.4-58
	MDMA	106[a]	N.D.	0.2-448[b]
Cathinones	Methylone	235 [202-264]	246 [194-308]	0.01-36[b]
	MDPV	29 [18-41]	14 [6.6-31]	0.02-30[b]
	α-PVP	21 [17-26]	28 [23-35]	0.01-2.1[b]
Hallucinogenic phenethylamines	2C-B	27 [24-30]	39 [33-48]	0.1-1.5[b]
	25B-NBOMe	2.4 [1.8-3.1]	3.3 [2.8-3.9]	0.004-0.3[b]
Piperazines	BZP	161 [129-205]	207 [152-288]	0.2-36[b]
	TFMPP	19 [16-22]	24 [22-26]	22-89[b]
	mCPP	32[a]	N.D.	1.7-85[b]
Arylcyclohexylamines	Ketamine	1.2[c]	N.D.	0.1-30[b]
	MXE	0.5[a,c]	N.D.	0.1-6.1[b]
Other	Cocaine	9.8 [8.7-11]	13 [11-15]	0.02-30

cathinones MDPV and α-PVP (IC$_{50}$ values of 29 μM and 21 μM, respectively) are ∼10-fold more potent than methylone, and ∼5 times more potent than amphetamine-type stimulants. This may be due to the addition of a pyrrolidine structure, a secondary cyclic amine. This notion is further supported by the potent inhibition by cocaine (IC$_{50}$ value 9.8 μM), which contains a tropane structure that includes a pyrrolidine structure. Again, the presence or absence of a methylenedioxy group (MDPV and α-PVP, respectively) did not significantly change IC$_{50}$ values, confirming earlier findings on the (lack of) contribution of the methylenedioxy group in MDMA compared to methamphetamine (Fig. 7).

In addition, other subclasses of (illicit) drugs also showed differences in wMFR IC$_{50}$ values of compounds within the same group. For example, the hallucinogenic phenethylamines 2C-B and 25B-NBOMe differ ∼10-fold in IC$_{50}$ values (27 μM vs 2.4 μM, respectively), while chemically only varying by the addition of a NBOMe (methoxybenzyl) group (Fig. 6). A comparable difference is seen between the piperazines BZP (IC$_{50}$ value of 161 μM), and TFMPP and mCPP (IC$_{50}$ values of 19 μM and 32 μM, respectively). This increase is most likely due to the addition of a halogen moiety on the phenyl ring, as halogens have been reported to enhance binding to target macromolecules (Dembinski et al., 2012).
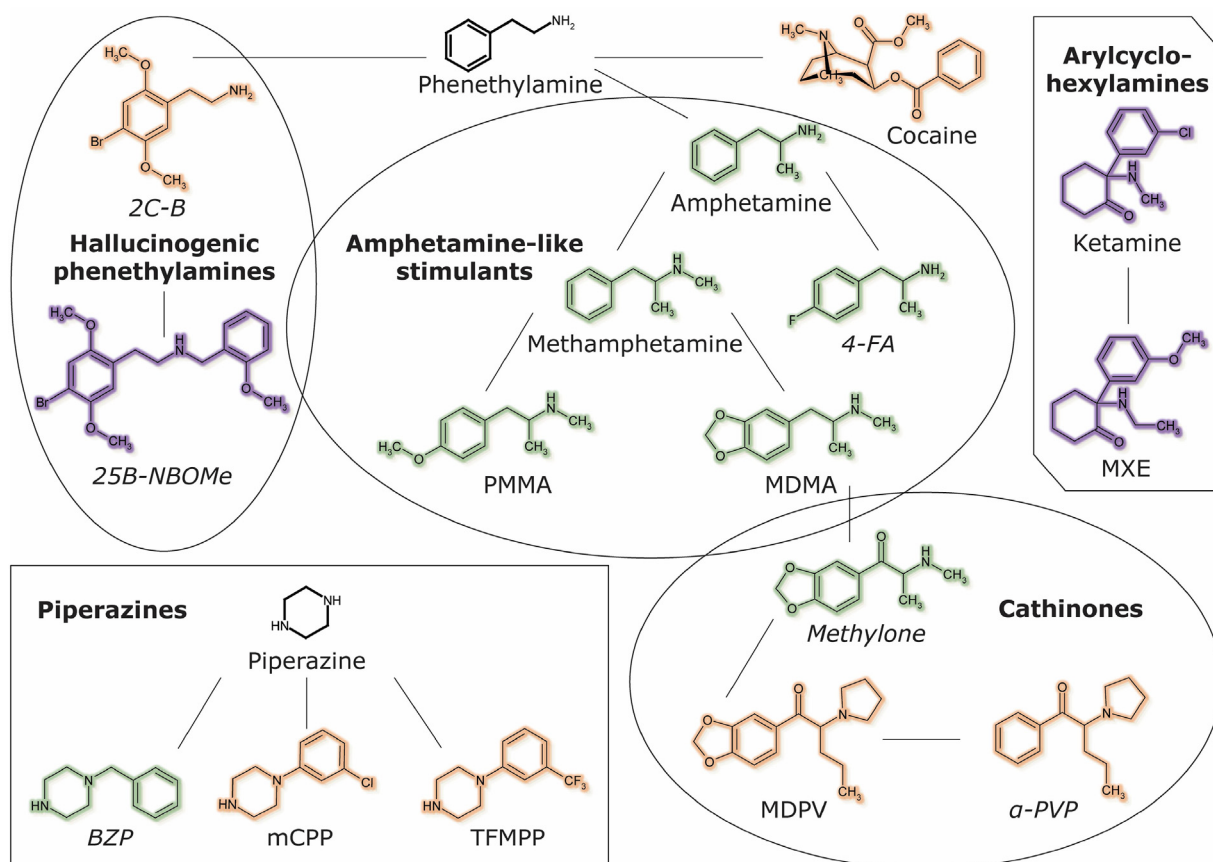
Fig. 7. Chemical structures of illicit drugs and NPS, categorized based on chemical similarities. Chemical classes depicted are amphetamine-type stimulants, hallucinogenic phenethylamines, cathinones, piperazines and arylcyclohexylamines. Compounds with comparable structures are linked by black lines. Colors represent the potency of a drug to affect neuronal activity: green (IC$_{50}$ values ∼100 μM and higher), orange (IC$_{50}$ values ∼10 μM) and purple (IC$_{50}$ values ∼1 μM). Drugs with IC$_{50}$ values not within or close to 2 times the estimated human brain concentration are listed in *italic*.

However, an increased potency to inhibit wMFR is not seen when comparing amphetamine and 4-FA.

Finally, of all compounds tested, the arylcyclohexylamines ketamine and methoxetamine (MXE) most potently inhibited wMFR with comparable IC$_{50}$ values of 1.2 μM and 0.5 μM, respectively (Table 3; Hondebrink et al., 2017). Others have reported a near complete inhibition of the MFR at 200 μM ketamine in a single concentration screening approach (McConnell et al., 2012). However, data on the effects of other drugs of abuse and NPS on wMFR and the wMBR from other laboratories, especially concentration-response curves, are rare, which hampers further comparison.

The present results, derived from an acute 30 min exposure, are unlikely to be confounded by effects on cell viability. Earlier studies showed no loss of viability when rat primary cortical cultures were exposed to up to 1 mM to structurally related compounds such as MDMA, amphetamine, 4-FA and MXE, whereas the piperazine analogue mCPP only showed minor effects on cell viability at 300 μM (Hondebrink et al., 2016). However, additional information on the reversibility of the effects and potential effects on cell viability following acute or prolonged exposure would aid in further pharmacological characterization of NPS. Nevertheless, our combined findings already provide a first step towards increasing knowledge on the relationship between chemical structures and drug effects for NPS. Still, more information on the effects on neuronal activity of various NPS belonging to different classes is needed for a robust (Q)SAR that could aid in risk reduction by *in silico* modelling.

Using the mwMEA, it is possible to quickly detect effects of NPS on neuronal activity as an integrated neuronal endpoint. When looking at IC$_{50}$ values for wMFR and wMBR, most drugs inhibited half of the spontaneous neuronal activity at concentrations relevant for human exposure (Table 3). However, the IC$_{50}$ values of 4-FA, methylone, α-PVP, 2C-B, 25B-NBOMe and BZP are well above the estimated human relevant brain concentration range. For BZP, this concentration is likely underestimated, since the brain partition factor was assumed to be 1 (brain concentration is the same as blood concentration) due to missing data. However, other piperazine derivatives show a rather high brain partition factor. Assuming a similar brain partition factor for BZP as for other piperazine derivatives would put the BZP-induced inhibition of neuronal activity (IC$_{50}$) in the range of concentrations relevant for human exposure (Hondebrink et al., 2018). Notably, the use of serum-containing medium in our experiments may have affected the free drug concentration. However, in our calculation of relevant human brain concentrations, we used blood concentrations of drug users in whom serum is also present.

Cortical cultures grown on mwMEA plates express a large number of functional targets and thus provide a useful integrated screening method for *in vitro* neurotoxicity testing (Vassallo et al., 2017; Hondebrink et al., 2016). MEA recordings thus represent the sum of the effects on all targets present in the model system. Nevertheless, some specific targets with a strict (extracortical) location in the brain, such as specific neurotransmitter receptors or transporters, are likely underrepresented in our *in vitro* model. This could also explain why some of the investigated drugs have IC$_{50}$

values for inhibition of neuronal activity above the estimated human brain concentrations. For example, monoamine reuptake transporters are inhibited by 4-FA, methylone, α-PVP and BZP at relevant concentrations (Hondebrink et al., 2018), while neuronal activity is not (Table 3). Similarly, 2C-B and 25B-NBOMe are presumed to primarily act as 5-HT$_2$ receptor agonists (Hondebrink et al., 2018), whereas in neonatal Wistar rat cortex only 5-HT$_{2A}$ and 5-HT$_{2C}$ receptor subtypes are expressed to some extent (Osredkar and Krzan, 2009). Consequently, risk and hazard characterization of NPS should involve integrated screening methods such as MEA recordings as well as dedicated assays to determine effects on specific targets such as monoamine reuptake transporters and serotonin/dopamine receptors (also see Hondebrink et al., 2018).

Overall, the number of NPS is increasing steadily while limited information is available regarding their pharmacology and toxicology. The 16 drugs tested in this study and our earlier (Hondebrink et al., 2017; 2016) studies belong to various drug classes and could therefore have different mechanisms of action, which would make targeted screening approaches laborious. Using mwMEA recordings, all 16 drugs tested showed concentration-dependent inhibition of spontaneous neuronal activity, with different potency but mostly within estimated human brain concentrations based on recreational use. mwMEA recordings may therefore provide a first step in linking chemical structures and drug classes to establish SARs, even before NPS appear on the drug market. Moreover, mwMEA recordings can thus provide an efficient integrated screening method that will aid in risk and hazard characterization of NPS, especially when the mechanism(s) of action are a priori unknown.

Conflict of interest

Acknowledgments

Appendix A. Supplementary data

Supplementary material related to this article can be found, in the online version, at doi:https://doi.org/10.1016/j.neuro.2018.03.007.

References

ACC, Australian Crime Commission, 2015. Illicit Drug Data Report 2013–14. http://apo.org.au/system/files/54723/apo-nid54723-56151.pdf (Accessed 28 September 2017).

Brajkovic, G., Babic, G., Stosic, J.J., Tomasevic, G., Rancie, D., Kilibarda, V., 2016. Fatal cocaine intoxication in a body packer. Vojnosanit. Pregl. 73, 198–201.

Chaturvedi, A.K., Cardona, P.S., Soper, J.W., Canfield, D.V., 2004. Distribution and optical purity of methamphetamine found in toxic concentration in a civil aviation accident pilot fatality. J. Forensic Sci. 49, 832–836.

Dembinski, R., Li, Y., Gundapuneni, D., Decker, A., 2012. Synthesis of beta-Halofurans. In: Iskra, J. (Ed.), Halogenated Heterocycles: Synthesis, Application and Environment. Springer Science & Business Media, Heidelberg, Dordrecht, London, New York pp. 65–100.

Dingemans, M.M.L., Schütte, M.G., Wiersma, D.M.M., de Groot, A., van Kleef, R.G.D.M., Wijnolts, F.M.J., Westerink, R.H.S., 2016. Chronic 14-day exposure to insecticides or methylmercury modulates neuronal activity in primary rat cultures. NeuroToxicology 57, 194–202.

EMCDDA, 2016. European monitoring centre for drugs an drug addictionRecent Changes in Europe's MDMA/ecstasy Market, . (Accessed 28 September 2017) http://www.emcdda.europa.eu/system/files/publications/2473/TD0116348ENN.pdf.

European Commission, 2014. Flash Eurobarometer Series No. 401 – Young People and Drugs. http://ec.europa.eu/commfrontoffice/publicopinion/flash/fl_401_en.pdf (Accessed 28 September 2017).

Giroud, C., Michaud, K., Sporkert, F., Eap, C., Augsburger, M., Cardinal, P., Mangin, P., 2004. A fatal overdose of cocaine associated with coingestion of marijuana, buprenorphine, and fluoxetine. Body fluid an tissue distribution of cocaine and its metabolites determined by hydrophilic interaction chromatography-mass spectrometry (HILIC-MS). J. Anal. Toxicol. 28, 464–474.

Hara, K., Nagata, T., Kimura, K., 1986. Forensic toxicologic analysis of methamphetamine and amphetamine in body materials by gas chromatography/mass spectrometry. Z. Rechtsmed. 96, 93–104.

Hondebrink, L., Zwartsen, A., Westerink, R.H.S., 2018. Effect fingerprinting of new psychoactive substances (NPS): What can we learn from in vitro data? Pharmacol. Ther. 182, 193–224.

Hondebrink, L., Kasteel, E.E.J., Tukker, A.M., Wijnolts, F.M.J., Verboven, A.H.A., Westerink, R.H.S., 2017. Neuropharmacological characterization of the new psychoactive substance methoxetamine. Neuropharmacology 123, 1–9.

Hondebrink, L., Verboven, A.H.A., Drega, W.S., Schmeink, S., de Groot, M.W.G.D.M., van Kleef, R.G.D.M., Wijnolts, F.M.J., de Groot, A., Meulenbelt, J., Westerink, R.H.S., 2016. Neurotoxicity screening of (illicit) drugs using novel methods for analysis of microelectrode array (MEA) recordings. NeuroToxicology 55, 1–9.

Irvine, R.J., Keane, M., Felgate, P., McCann, U.D., Callaghan, P.D., White, J., 2006. Plasma drug concentrations and physiological measures in 'dance party' participants. Neuropsychopharmacology 31, 424–430.

Jones, A.W., Holmgren, A., Kugelberg, F.C., 2008. Driving under the influence of central stimulant amines: age and gender differences in concentrations of amphetamine, methamphetamine, and ecstasy in blood. J. Stud. Alcohol Drugs 69, 202–208.

Kiely, E., Lee, C.J., Marinetti, L., 2009. A fatality from an oral ingestion of methamphetamine. J. Anal. Toxicol. 33, 55–560.

Kiszka, M., Madro, R., 2004. Alcohol and cocaine - presentation of a fatal case. Prob. Forensic Sci. 60, 117–129.

Kojima, T., Une, I., Yashiki, M., Noda, J., Sakai, K., Yamamoto, K., 1984. A fatal methamphetamine poisoning associated with hyperpyrexia. Forensic Sci. Int. 24, 87–93.

MacLeod, K., Pickering, L., Gannon, M., Greenwood, S., Liddell, D., Smith, A., Johnstone, L., Burton, G., 2016. Understanding the Patterns of Use, Motives, and harms of New Psychoactive Substances in Scotland. http://www.gov.scot/Resource/0051/00510607.pdf (Accessed 28 September 2017).

McConnell, E.R., McClain, M.A., Ross, J., LeFew, W.R., Shafer, T.J., 2012. Evaluation of multi-well microelectrode arrays for neurotoxicity screening using a chemical training set. NeuroToxicology 33, 1048–1057.

Melega, W.P., Cho, A.K., Harvey, D., Lacan, G., 2007. Methamphetamine blood concentrations in human abusers: application to pharmacokinetic modeling. Synapse 61, 216–220.

Nicolas, J., Hendriksen, P.J.M., van Kleef, R.G.D.M., de Groot, A., Bovee, T.F.H., Rietjens, I.M.C.M., Westerink, R.H.S., 2014. Detection of marine neurotoxins in food safety testing using a multielectrode array. Mol. Nutr. Food Res. 58, 2369–2378.

Novellino, A., Scelfo, B., Palosaari, T., Price, A., Sobanski, T., Shafer, T.J., Johnstone, A.F., Gross, G.W., Gramowski, A., Schroeder, O., Jügelt, K., Chiappalone, M., Benfenati, F., Martinoia, S., Tedesco, M.T., Defranchi, E., D'Angelo, P., Whelan, M., 2011. Development of micro-electrode array based tests for neurotoxicity: assessment of interlaboratory reproducibility with neuroactive chemicals. Front. Neuroeng. 4 (April (4)) doi:http://dx.doi.org/10.3389/fneng.2011.00004 eCollection 2011.

Osredkar, D., Krzan, M., 2009. Expression of serotonin receptor subtypes in rat brain and astrocyte cell cultures: an age- and tissue-dependent process. Period. Biol. 111, 129–135.

Pálenícek, T., Malíková, M., Rohanová, M., Novák, T., Horácek, J., Fujáková, M., Höschl, C., 2011. Behavioral, hyperthermic and pharmacokinetic profile of para-methoxymethamphetamine (PMMA) in rats. Pharmacol. Biochem. Behav. 98, 130–139.

Poklis, A., Maginn, D., Barr, J., 1987. Tissue disposition of cocaine in man: a report of five fatal poisonings. Forensic Sci. Int. 33, 83–88.

Poklis, A., Mackell, M.A., Graham, M., 1985. Disposition of cocaine in fatal poisoning in man. J. Anal. Toxicol. 9, 227–229.

Puia, G., Gullo, F., Dossi, E., Lecchi, M., Wanke, E., 2012. Novel modulatory effects of neurosteroids and benzodiazepines on excitatory and inhibitory neurons excitability: a multi-electrode array recording study. Front. Neural Circuits 6, 1–17.

Rickli, A., Hoener, M.C., Liechti, M.E., 2015. Monoamine transporter and receptor interaction profiles of novel psychoactive substances: para-halogenated amphetamines and pyrovalerone cathinones. Eur. Neuropsychopharmacol. 25, 365–376.

Rohanova, M., Balikova, M., 2009. Studies on distribution and metabolism of para-methoxymethamphetamine (PMMA) in rats after subcutaneous administration. Toxicology 259, 61–68.

Saito, T., Takeichi, S., Nakajima, Y., Yukawa, N., Osawa, M., 1996. Fatal methamphetamine poisoning in police custody. J. Clin. Forensic Med. 3, 183–185.

Senna, M.C., Augsburger, M., Aebi, B., Briellmann, T.A., Donzé, N., Dubugnon, J.L., Iten, P.X., Staub, C., Sturm, W., Sutter, K., 2010. First nationwide study on driving under the influence of drugs in Switzerland. Forensic Sci. Int. 198, 11–16.

Simmler, L.D., Buser, T.A., Donzelli, M., Schramm, Y., Dieu, L.H., Huwyler, J., Chaboz, S., Hoener, M.C., Liechti, M.E., 2013. Pharmacological characterization of designer cathinones in vitro. Br. J. Pharmacol. 168, 458–470.

Soussan, C., Kjellgren, A., 2016. The users of novel psychoactive substances: online survey about their characteristics, attitudes and motivations. Int. J. Drug Policy 32, 77–84.

Steentoft, A., Simonsen, K.W., Linnet, K., 2010. The frequency of drugs among Danish drivers before and after the introduction of fixed concentration limits. Traffic Inj. Prev. 11, 329–333.

Strickland, J.D., Martin, M.T., Richard, A.M., Houck, K.A., Shafer, T.J., 2018. Screening the ToxCast phase II libraries for alterations in network function using cortical neurons grown on multi-well microelectrode array (mwMEA) plates. Arch. Toxicol. 92, 487–500.

UNODC, 2017. United nations office on drugs and crimeWorld Drug Report 2017, . . (Accessed 28 September 2017) https://www.unodc.org/wdr2017/index.html.

Valdivia, P., Martin, M., LeFew, W.R., Ross, J., Houck, K.A., Shafer, T.J., 2014. Multi-well microelectrode array recordings detect neuroactivity of ToxCast compounds. NeuroToxicology 44, 204–217.

Van der Gouwe, D., Rigter, S., 2017. Annual Report 2016, Drugs Information and Monitoring System (DIMS). https://assets-sites.trimbos.nl/docs/27b4c407-3fa0-44ef-891b-9ca90ba335dc.pdf (Accessed 28 September 2017).

Vassallo, A., Chiappalone, M., De Camargos Lopes, R., Scelfo, B., Novellino, A., Defranchi, E., Palosaari, T., Weisschu, T., Ramirez, T., Martinoia, S., Johnstone, A.F.M., Mack, C.M., Landsiedel, R., Whelan, M., Bal-Price, A., Shafer, T.J., 2017. A multi-laboratory evaluation of microelectrode array-based measurements of neural network activity for acute neurotoxicity testing. NeuroToxicology 60, 280–292.

Vevelstad, M., Oiestad, E.L., Middelkoop, G., Hasvold, I., Lilleng, P., Delaveris, G.J.M., Eggen, T., Morland, J., Arnestad, M., 2012. The PMMA epidemic in Norway: comparison of fatal and non-fatal intoxications. Forensic Sci. Int. 219, 151–157.

Wood, D.M., Sedefov, R., Cunningham, A., Dargan, P.I., 2015. Prevalence of use and acute toxicity associated with the use of NBOMe drugs. Clin. Toxicol. (Phila) 53, 85–92.

Zwartsen, A., Verboven, A.H.A., van Kleef, R.G.D.M., Wijnolts, F.M.J., Westerink, R.H.S., Hondebrink, L., 2017. Measuring inhibition of monoamine reuptake transporters by new psychoactive substances (NPS) in real-time using a high-throughput, fluorescence-based assay. Toxicol. In Vitro 45, 60–71.